

Haijun Hu
 Harvard University, Cambridge, Massachusetts
 L. Larrabee Strow
 University of Maryland at Baltimore County, Baltimore, Maryland
 David W. Keith, and James G. Anderson
 Harvard University, Cambridge, Massachusetts

1. Introduction

Remote sounding of atmospheric temperature profiles, which is of paramount importance to numerical weather forecasting, has been conducted routinely with the 15- μm CO_2 band using low spectral resolution satellite remote sensors. Next generation atmospheric sounders, such as the Atmospheric Infrared Sounder, AIRS (Aumann and Pagano 1994), is also designed to use the 15- μm CO_2 band, but in addition will have spectral channels in the 4.3- μm CO_2 R branch. This region is useful because the weighting functions are quite sharp (partially due to the lack of interfering hot bands and isotopes) and because the Planck function is more sensitive to the temperature in the short wave. AIRS has a nominal spectral resolution of 2 cm^{-1} in this region, thus producing a good number of channels with sharp weighting functions.

Like remote sounding using the 15- μm CO_2 band, implementation of the 4.3- μm band sounding requires an accurate forward transmittance model for temperature retrieval. The well-known extreme sub-Lorentz behavior of the CO_2 lineshape in this region is difficult to model, especially inside the bandhead between lines, which is where the best sounding channels are located. Moreover, there are very few studies of the lineshape at low temperatures relevant for atmospheric sounding. Thus, validation of forward model assumptions with in-flight measurements is an important step toward improvements of model and temperature retrieval.

Here we present our approach and preliminary findings from a recent field campaign using a newly developed high-resolution Interferometer for Emission and Solar Absorption (INTESA) flown on the NASA ER-2. The observed radiances and transmittances are compared to computed quantities using a new pseudo line-by-line algorithm, kCARTA (Strow et al. 1998). kCARTA uses compressed look-up tables for computation of transmittances and radiances which were derived from the GENLN2 line-by-line code (Edwards

1992), which uses a parameterization of the 4.3- μm CO_2 lineshape developed by Cousin et al. (1985).

2. Experiments

INTESA measures spectra of both atmospheric emission and solar absorption with an unapodized resolution of 0.48 cm^{-1} and, hence, allows direct comparisons of measurements from both atmospheric emission and solar absorptions. These measurements were accompanied by high-accuracy *in situ* measurements of CO_2 and water vapor, which can be used to validate radiative transfer for moisture sounding (to be reported later). Here, we limit discussion to the 4.3- μm CO_2 band.

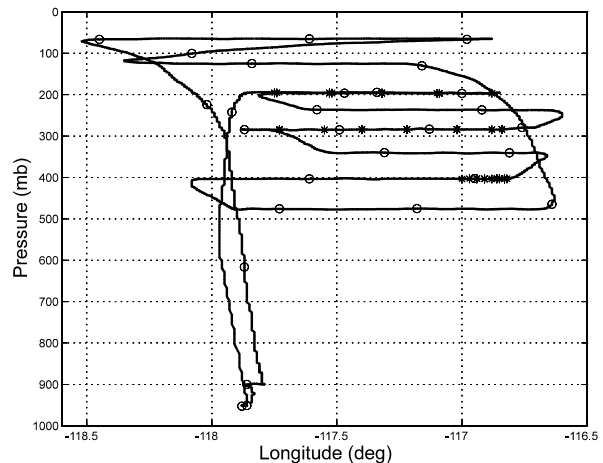


Figure 1: A stair-step flight profile over NASA Dryden Flight Research Center, CA, in November 1998. Open circles mark the 10-min time interval and asterisks indicate the location where solar absorption spectra were taken and used in this analysis.

The instrument employs a software-controlled sun-tracker which locks onto the sun and directs the solar beam into the Fourier Transform Spectrometer (FTS). To test radiative transfer using solar absorption, a series of stair-step, horizontal flight legs were executed with the NASA ER-2 (see Figure 1 for a flight trajectory) in

Corresponding author address: Haijun Hu, Harvard University, Department of Earth and Planetary Sciences and Department of Chemistry, Cambridge, MA 02138; e-mail: hu@huarp.harvard.edu.

November 1998. Each of the horizontal legs took about 20 min and the entire flight took approximately four hours to complete. Clear sky and stable meteorological conditions, desirable for the experiments here, were achieved by closely monitoring meteorological satellite observations and local forecasts. Radiosonde data from nearby sites were used to give the vertical atmospheric profiles. During this flight, the sun-tracker did not lock consistently for all the horizontal legs due to changes in solar angle viewed by the sun-tracker and engineering issues. However, three horizontal legs produced fairly stable solar spectra for analysis. The three legs used for this analysis are marked with asterisks in Figure 1.

Terrestrial emission spectra were measured with INTESA looking downward from the aircraft. Periodic calibrations were executed in-flight by looking at three blackbodies with accurately controlled temperatures bracketing the temperatures of the scene below. To avoid the inhomogeneity of land surface emissivity, the emission data were taken from a flight westward of the southern California coast. Vertical temperature profiles along the flight track were retrieved by a statistical regression model using radiance measurement from the 15- μm band of CO_2 . In addition, radiosonde profiles taken by nearby coastal stations were collected.

3. Data Uncertainty and Model Sensitivity

3.1 Comparison of Data with Model

Measured interferograms are transformed by Fast Fourier Transform (FFT). Phase correction, spectral calibration, and solar angle corrections are subsequently applied. The individual spectrum is then normalized against its peak values in nearby windows. This empirical process can largely eliminate the unknown scattering effects, such as those due to aerosol and possibly sub-visible cirrus, which do not have strong wavelength dependence. Corrected spectra from different altitudes are then ratioed to derive the effective layered transmittance resolvable by the spectrometer. Line-by-line calculations are done similarly with sounding profiles and are reduced to the instrumental resolution for comparison.

Figure 2 compares the instrumental data with calculations. The comparisons are made for three atmospheric layers in the upper troposphere, covering the slabs of 196.4-284.2, 284.2-403.3, and 196.4-403.3 mb, respectively. In the primary temperature sounding channels located at 2383-2400 cm^{-1} , the transmittances are well situated for measurements and comparison. A maximum difference of ~ 0.06 in transmittance is seen from the two thicker layers whereas the difference for the thinner layer (top panel) is considerably smaller. The model atmosphere is consistently more transparent than the measurement, suggesting that the model may have underestimated the CO_2 absorption throughout the band, but overall, the agreement between the two is quite good given the magnitude of the differences depicted here and the uncertainties to be discussed next.

Beyond 2420 cm^{-1} , the atmosphere is very transparent, while below 2381-2383 cm^{-1} (depending on the altitude of measurement), the absorptions are too strong to be quantified by the method here due to the still large amount of CO_2 in the upper troposphere. In general, flight legs at higher altitudes are preferable in resolving spectral structures closer to the band center, while legs at lower altitude are better suited for deriving transmittance of the band wings. In addition, the lower flight legs are especially useful for water vapor absorption measurements.

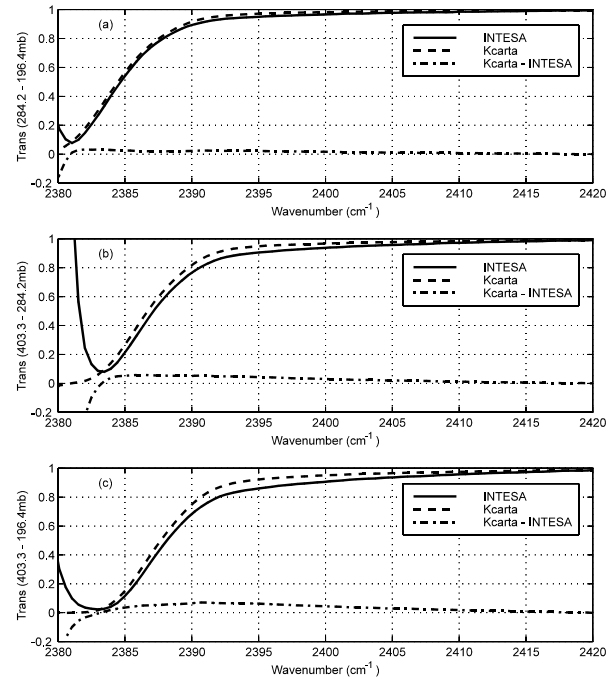


Figure 2: Comparison of layered atmospheric transmittance derived from INTESA solar absorption measurement (solid lines) with calculations using kCARTA (dashed lines). The differences are indicated in dot-dashed lines. Transmittances of three atmospheric layers are shown in (a), (b), and (c), respectively.

Comparison of the emission mode measurement with calculations (expressed in brightness temperature) is given in Figure 3. We performed calculations for both the radiosonde and retrieved profiles and found the differences were generally small (less than 1 K) in 2380-2395 cm^{-1} , but becomes larger beyond 2395 cm^{-1} . Figure 3 shows the comparison with the retrieved profile. It is seen that the model is colder than the measurement by a few degrees (1-7 K) for wavenumber between 2380-2395 cm^{-1} . This indicates that the modeled absorption is too strong, either due to lineshape errors (the R-branch bandhead lineshape is extremely sub-Lorentzian), or possibly due to inaccurate modeling of the temperature dependence. This seems to contradict

what we saw from the solar absorption measurement, which suggests a weaker model absorption, but it will soon become clear that the absorption measurement made here may not be good enough to tell the difference. It should also be noted that the two measurements were made at locations with distinct climates: the absorption measurement over Dryden Flight Research Center of desert climate, and the emission measurement off the coast of southern California, which is maritime. These two locations may have very different aerosol loading and contribute to the difference in solar scattering, but its significance is less obvious.

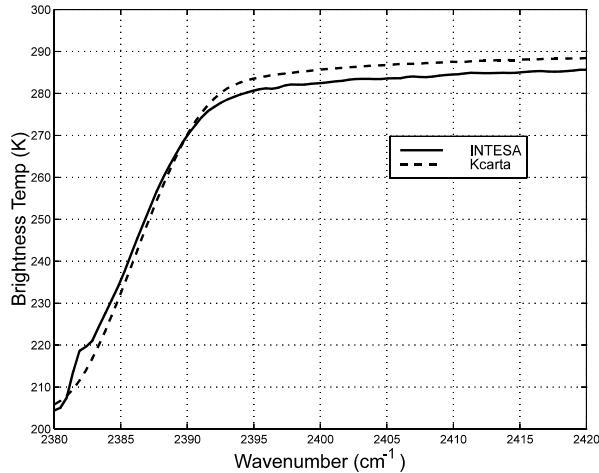


Figure 3: Comparison of brightness temperatures observed by the instrument and calculated by the model, with their differences shown in (b).

Beyond 2390 cm^{-1} , the difference is very small when we use the retrieved temperature profile but becomes large if we use the radiosonde profile. The latter difference is most likely due to an incorrect sea surface temperature, primarily due to mismatches of flight track with radiosonde launching site or mismatch of time (the so-called co-location problem). The Vandenberg sounding site used here is about 150 km north of the flight, with a temporal mismatch of about an hour. In addition, this station is most likely to be affected by the land. We will next discuss the overall measurement uncertainty, in light of model sensitivity.

3.2 Measurement Uncertainty and Model Sensitivity

We discuss the measurement uncertainty first. The estimated uncertainty of the derived transmittance is about 3-5% for the high-transmission bands and it is considerably worse for bands with low transmission ($< 2390\text{ cm}^{-1}$). This value is based on the variation of signal-intensity detected by the instrument from individual legs. For both modes of operation, a signal to noise ratio of ~ 500 is achieved by co-adding. Radiosonde temperature measurement typically has an accuracy of better than 1 K, but it degrades for low pressures due to inac-

curacy in pressure measurement (Nash and Schmidlin, 1987). Uncertainty of temperature due to the co-location problem can be significantly larger than 2 K below 800 mb although it typically becomes smaller above this level. Our retrieved temperature accuracy is believed to be around 1 K based on tests with a large radiosonde data set. In particular, the retrieved surface temperature shown in Figure 3 (using the $15\text{-}\mu\text{m CO}_2$ measured by a different detector) is within 0.3 K of that derived from the windows beyond 2420 cm^{-1} . This agreement demonstrates the overall accuracy of the instrument, making it a self-sufficient tool for applications as shown here because it does not need to co-locate with a radiosonde.

A typical CO_2 drop of ~ 5 ppmv, from its surface value of 365 ppmv to its typical lowerstratospheric value of 360 ppmv, has been measured with an in situ instrument flying on the ER-2. An estimated uncertainty of 0.02 for sea surface emissivity is based on Smith et al. (1996).

In order to understand the degree to which the discrepancy between the model and the measurements can be explained by uncertainties due to imperfect instrumentation or modeling assumptions, we have performed the following sensitivity study based on modeling efforts. The perturbations we made include: (1) 5 mb in aircraft flight altitude, (2) 5 ppmv of CO_2 , (3) black surface versus non-black surface, with a 2% change of surface emissivity, (4) 1 K Gaussian noise added to the sounding profile, (5) contributions due to reflected solar radiation, (6) contributions due to downward thermal radiation, (7) 2% change of non-black surface emissivity, and (8) the combination of (5)–(7).

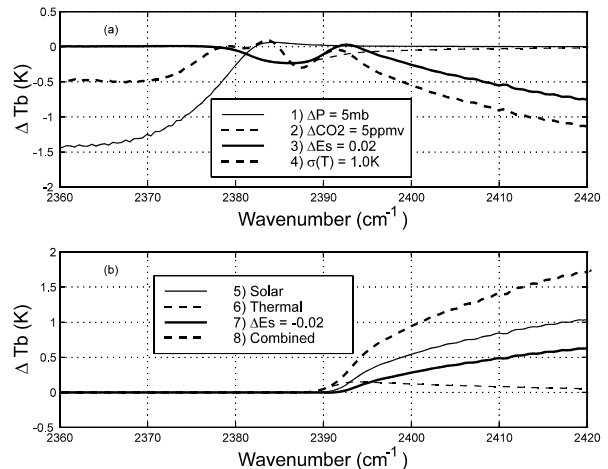


Figure 4: Model sensitivity expressed in changes of brightness temperature as would be observed from 55 mb. See text for a list of perturbations.

The results from the sensitivity study are shown in Figure 4, expressed as the changes in spectrally-resolved brightness temperature as would be detected by a perfect instrument at the ER-2 cruise altitude of 20 km, or 55 mb. An inaccuracy of pressure measurement by 5 mb can only affect brightness temperatures in the near-band-center region below 2380 cm^{-1} , which is not our

major concern here; a 5 ppmv change of CO₂ will lead to a maximum brightness temperature change of about 0.25 K between 2380-2390 cm⁻¹ with virtually no change elsewhere; the most dramatic change due to the switch between black surface and non-black surface is seen beyond 2395 cm⁻¹, where the influence of reflected solar radiation is becoming increasingly important, and it is otherwise similar to the 5-ppmv change of CO₂. The biggest change, however, is due to the addition of a 1 K noise to the sounding profile, with the most sensitive perturbation seen from the surface temperature, which dominates the sign of change for the entire band and alters the window region the most.

In contrast, the contributions due to reflected solar, downward thermal, and a decrease of non-black surface emissivity have similar characteristics and are essentially additive.

4. Discussion and Conclusion

We have proposed and tested a comprehensive method to validate radiative transfer using both solar absorption and thermal emission measurements with the newly developed Interferometer for Emission and Solar Absorption (INTESA). Based on our test flight and preliminary analysis, we demonstrated that the method is feasible, producing good results, but further improvements of the instrument operation and refinement of data analysis are still needed. Specifically, we found that the solar absorption measurement at its current stage may not be stable enough to derive, with certainty, the desired layered transmittances. Or more quantitatively, we found that the differences between the measured transmittance and the calculated transmittance are as big as the uncertainties in the solar measurement. Therefore, improvement toward more stable locking of the solar signal is necessary for future measurements in order to obtain quantitative agreement.

On the other hand, the differences shown by the emission model comparison are clearly beyond the measurement uncertainty discussed here, and we believe are real. The differences beyond 2395 cm⁻¹ can be due to uncertainty of surface emissivity, reflected solar or thermal emission, but they are most likely to be dominated by mismatches of flight track with radiosonde or inaccuracy in surface temperature measurement. Those factors, however, cannot explain the discrepancies between 2380-2395 cm⁻¹, which originate from the levels above the boundary layer. Our survey of limited radiosonde profiles bracketing the flight time and area exhibits stable temperatures above 800 mb, i.e., the altitude where the majority of the 2380-2395-cm⁻¹ channels are most responsive. Moreover, by using our retrieved temperature profiles, we have essentially eliminated the major uncertainties such as those due to collocation or unknown surface temperatures. The advantage of such applications is evident. Therefore, we come to the conclusion that the current model has significantly overestimated CO₂ absorption in the 4.3- μ m R branch. Further work on model improvement will be reported in near future.

5. References

- Aumann, H. H., and R. J. Pagano, 1994: Atmospheric infrared sounder on the Earth Observing System. *Opt. Eng.*, **33**, 776-784.
- Cousin, C., R. Le Doucen, C. Boulet, and A. Henry, 1985: Temperature dependence of the absorption in the region beyond the 4.3- μ m band head of CO₂. 2: N₂ and O₂ broadening. *Appl. Opt.*, **22**, 3899-3907.
- Edwards, D. P., 1992: GENLEN2: A general line-by-line atmospheric transmittance and radiance model: Version 3.0 description and users guide. NCAR Tech. Note, NCAR/TN-367+STR, Boulder, CO., 147 pp.
- Rinsland, C. P., and L. L. Strow, 1988: Line mixing effects in solar occultation spectra of the lower stratosphere: measurements and comparisons with calculations for the 1932-cm⁻¹ CO₂ Q branch. *Appl. Opt.*, **28**, 457-464.
- Nash, J., and F. J. Schmidlin, 1987: WMO international radiosonde comparison, instruments and observing methods. WMO Rep. 30, WMO/TD-No. 195, 103pp.
- Smith, W. L., R. O. Knuteson, H. E. Revercomb, W. Feltz, H. B. Howell, W. P. Menzel, N. R. Nalli, O. Brown, J. Brown, P. Minnett, and W. McKeown, 1996: Observations of the infrared radiative properties of the ocean - implications for measurement of sea surface temperature via satellite remote sensing. *Bull. Amer. Meteor. Soc.*, **77**, 41-51.